Insertion of Sc^+ into H_2: The First Example of Cluster-Mediated σ-Bond Activation by a Transition Metal Center

John E. Bushnell, Paul R. Kemper, Philippe Maitre,† and Michael T. Bowers*

Contribution from the Department of Chemistry, University of California, Santa Barbara, California 93106

Received May 4, 1994®

Abstract: Dissociation energies and entropies for H_2 loss from $Sc^+(H_2)_n$ clusters (n = 1–5) have been determined via temperature-dependent equilibrium measurements. The measured dissociation energies ($D_0 = -\Delta H_0^\circ$) are 6.4 ± 0.5, 5.4 ± 0.3, and 5.0 ± 0.4 kcal/mol for n = 2–4, respectively, and ~4.5 kcal/mol for n = 5. For n = 1, two isomeric forms are identified: the electrostatic complex Sc^+H_2 with D_0 = 2.1 ± 0.5 kcal/mol and the inserted complex H–Sc^+–H with D_0 = 5.5 ± 0.3 kcal/mol. These thermodynamic data are compared with other results. Both experimental and theoretical analyses of the data indicate the Sc^+ ion is inserted into the first H_2 ligand, although the rate (k = 3–13 × 10^{-17} cm^3/s) is very slow. This rate constant has a negative temperature dependence which is incompatible with a simple insertion energy barrier. A reaction mechanism involving the uninserted $Sc^+(H_2)_n$ clusters is proposed to explain the rate data and is supported by selected *ab initio* calculations. Optimized structures and vibrational frequencies (calculated at the MP2 level) are also given for the subsequent clusters (n = 2–4) along with the calculated heats of formation. A solvation shell of 6 is observed for Sc^+ (two H-atom and four H_2 ligands) consistent with other first-row metals.

Introduction

In the past several years, the coordination of dihydrogen with several first row transition metal ions has been explored both theoretically and experimentally. In our laboratory, we have explored these systems by forming state selected transition metal and alkali ions[1,2] and clustering them sequentially with up to seven H_2 molecules. By measuring equilibrium constants as a function of temperature, we have been able to determine accurate binding energies for individual H_2 ligands. Ions studied previously include $[Co^+]$,[3] $[V^+]$,[4] $[Na^+]$,[5] and $[K^+]$.[5] In all these systems, our experimental binding energies have agreed well with theory, where available, and all are considered to be cases of non-classical dihydrogen addition.

This work has stimulated substantial theoretical interest in an effort to understand the trends observed experimentally.[6-10] (See ref 10 for recent reviews.) The theoretical investigations have identified a number of factors that affect the bonding between the metal center and the H_2 ligands in these clusters. In all the systems which we have previously investigated experimentally, the H_2 ligands are bound mainly by electrostatic forces, and the H_2 bond length is only slightly perturbed from the isolated H_2 molecule. Nonetheless, rearrangements of valence electrons occur and produce a substantial increase in the M^+–H_2 binding energies.[4,5] Such electron rearrangements include $d\pi(M^+) \rightarrow \sigma^*(H_2)$ donation, 3d–4s hybridization in the M^+ ion, and $\sigma(H_2) \rightarrow sd\sigma(M^+)$ donation. Theoretical investigations have shown all of these to contribute (in varying degrees) to the binding between first row transition metal ions and dihydrogen. We refer to these effects as covalent interactions (although the H_2 ligand remains largely unperturbed) to distinguish them from the purely electrostatic forces that are also present (the point charge induced dipole and point charge quadrupole attractions between M^+ and H_2 as well as the quadrupole–quadrupole repulsion between ligands).

The reaction of Sc^+ with H_2 provided a possible exception to the largely electrostatic M^+–H_2 clustering observed so far. The Sc^+ ion (^3D 4s3d ground state) is by far the most reactive of the first row transition metal ions. It is known to dehydrogenate ethane and higher alkanes as well as ethylene and acetylene.[11,12] The exothermic insertion of Sc^+ into H_2, forming two Sc–H σ bonds, was first predicted by Tolbert and Beauchamp,[13] based upon the observation that the reaction of Sc^+ with formaldehyde (eq 1)is exothermic at a relative kinetic energy of 0.5 eV. This

$$Sc^+ + CH_2O \rightarrow ScH_2^+ + CO \qquad (1)$$

ability to form metal–hydride bonds was attributed to the fact that the 3d4s configuration of Sc^+ allows the formation of two equivalent sd hybrid bonding orbitals and greatly reduces the loss of exchange energy on the metal associated with the formation of two Sc^+–H σ bonds.

By measuring endoergic reaction thresholds, Armentrout and co-workers were able to determine first and second Sc^+–H bond strengths.[11,14,15] Subsequent theoretical work by both Rappe and Upton[16] and Swaisgood and Harrison[17] found the Sc^+–H_2 ground state to be an inserted species. Both groups calculated very similar

† Permanent address: Laboratoire de Chimie Theorique, Batiment 490, Universite de Paris Sud, 91405 Orsay Cedex, France.

* Abstract published in *Advance ACS Abstracts*, September 15, 1994.

(1) Kemper, P. R.; Bowers, M. T. *J. Phys. Chem.* **1991**, *95*, 5134.
(2) Bowers, M. T.; Kemper, P. R.; von Helden, G.; van Koppen, P. A. M. *Science* **1993**, *260*, 1446.
(3) Kemper, P. R.; Bushnell, J.; von Helden, G.; Bowers, M. T. *J. Phys. Chem.* **1993**, *97*, 52.
(4) Bushnell, J. E.; Kemper, P. R.; Bowers, M. T. *J. Phys. Chem.* **1993**, *97*, 11628.
(5) Bushnell, J. E.; Kemper, P. R.; Bowers, M. T. *J. Phys. Chem.* **1994**, *98*, 2044.
(6) Bauschlicher, C. W.; Partridge, H.; Langhoff, S. R. *J. Phys. Chem.* **1992**, *96*, 2475.
(7) Maitre, P.; Bauschlicher, C. W., manuscript in preparation.
(8) Maitre, P.; Bauschlicher, C. W. *J. Phys. Chem.* **1993**, *97*, 11912.
(9) Perry, J. K.; Ohanessian, G.; Goddard, W. A., III *J. Phys. Chem.* **1993**, *97*, 5238.
(10) (a) Bauschlicher, C. W., Jr.; Langhoff, S. R.; Partridge, H. *Modern Electronic Structure Theory*, submitted for publication. (b) Bauschlicher, C. W.; Langhoff, S. R. *Int. Rev. Phys. Chem.* **1990**, *9*, 149.
(11) Sunderlin, L.; Aristov, N.; Armentrout, P. B. *J. Am. Chem. Soc.* **1987**, *109*, 78.
(12) Tonkyn, R.; Ronan, M.; Weisshaar, J. C. *J. Phys. Chem.* **1988**, *92*, 92.
(13) Tolbert, M. A.; Beauchamp, J. L. *J. Am. Chem. Soc.* **1984**, *106*, 8117.
(14) Elkind, J. L.; Sunderlin, L. S.; Armentrout, P. B. *J. Phys. Chem.* **1989**, *93*, 3151.

0002-7863/94/1516-9710$04.50/0

bond energies, geometries, and vibrational frequencies. The very detailed analyses by Rappe and Upton of the possible reaction paths indicated that the low lying first excited state (^{1}D 3d4s) actually leads adiabatically to the inserted product through an avoided crossing with the third excited state (^{1}D 3d^2). Furthermore, Rappe and Upton also estimated the efficiency of the spin–orbit coupling between surfaces of ScH_2^+ that correlate to the ground ^{3}D and first excited ^{1}D states of Sc^+. This calculation indicated that formation of the inserted H–Sc^+–H ion was probably exothermic with respect to the Sc^+ ground state but that a large barrier to reaction from the ground state was present (~20 kcal/mol). The reaction of Sc^+ at thermal energies was thus predicted to be extremely slow.

The reaction of Sc^+ with H_2 seemed to involve a number of questions that could be answered by our equilibrium experiment. Foremost among them was whether insertion could actually occur at low energies. In order to answer this and other questions, we have accurately determined the enthalpies and entropies associated with the formation of $Sc^+(H_2)_n$ clusters (n = 1–4) by temperature-dependent equilibrium measurements. In addition, we have carefully measured the approach at equilibrium for formation of the ScH_2^+ species from Sc^+ and H_2 and from analysis of the data obtained rate constants as a function of temperature. The behavior observed is strongly inconsistent with the formation of an electrostatically bound Sc^+–H_2 complex as the approach to equilibrium is exceedingly slow while for all other systems equilibrium occurs at a rate too rapid to measure in our apparatus. However, a negative temperature dependence of the rate constant is observed, making formation of an inserted H–Sc^+–H species via a barrier process unlikely. In this paper we will discuss a "cluster assisted" insertion mechanism that can account for all of the experimental data; we also support this mechanism with ab initio calculations. To our knowledge this is the first such mechanism observed for σ-bond activation by transition metal centers.

Experimental Technique and Data Analysis

The instrument,[18] the equilibrium experiment, and the data analysis methods[3,5,19] all have been described previously. Sources of error have also been discussed extensively.[3] A brief overview is given here with emphasis on the differences encountered in these experiments.

The Instrument. The Sc^+ ions are formed via surface ionization of $ScCl_3$ on a hot filament (Re ribbon T ~2500 K). $ScCl_3$ vapor is produced by heating a sample of $ScCl_3$ powder in a small oven attached to the ion source. The nascent ions are accelerated to 5 keV, mass selected with a double focusing, reverse geometry mass spectrometer, decelerated to approximately 3–5 eV, and injected into a reaction cell containing H_2 at about 1 × 10^{17} molecule/cm^3 (3 Torr at 300 K). The ions are quickly thermalized via collisions with the H_2 and move through the 4 cm long reaction cell under the influence of a small, uniform electric field. The electric field is kept small to avoid perturbing the ion thermal energy (E/N < 2.5 × 10^{-17} cm^2·V). The H_2 pressure in the reaction cell is monitored directly with a capacitance manometer. Cell temperatures are varied using a flow of heated or cooled N_2, and temperatures are measured using a thin-film platinum resistor suspended in the H_2 bath gas. Ions exiting the cell are accelerated slightly (2–5 eV), quadrupole mass analyzed, and collected with standard ion counting techniques. The quadrupole is scanned by a computer over the mass range of interest and the baseline-resolved peaks are then integrated to give the relative ion intensities.

The Equilibrium Experiment. After the temperature and H_2 pressure are observed to be stable within the reaction cell, product/parent ion ratios are measured as a function of reaction time. This time is varied by changing the drift voltage across the cell. As the drift time is increased, the product/parent ion ratios eventually become constant, indicating that equilibrium has been reached. The $Sc^+ + H_2 \rightleftharpoons Sc^+(H_2)$ system required unusually long times to attain equilibrium (see below). These reactions were probed out to 3–8 ms (4–12 × 10^5 collisions) to ensure equilibrium had been established. This procedure also ensures that the drift field is not significantly perturbing the ion thermal kinetic energy. For selected experiments, the pressure of H_2 was varied by a factor of three with no significant change observed in ΔG_T°.

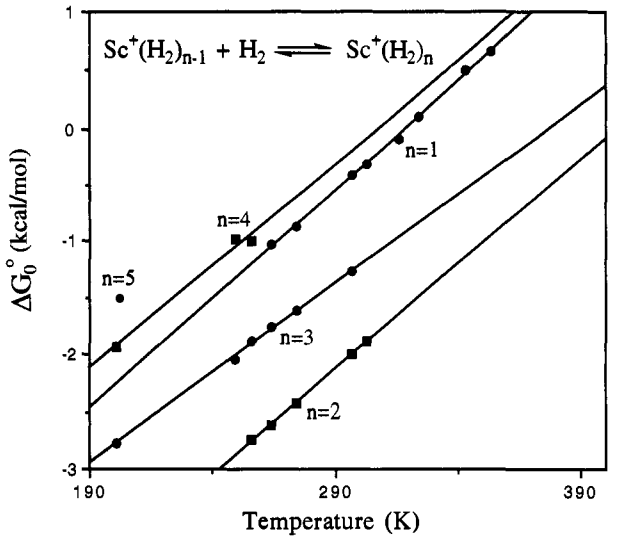

Figure 1. Plots of ΔG° *vs* temperature for the sequential addition of H_2 molecules to ground state Sc^+ ions. The values of ΔG° are deduced from measured equilibrium constants as described in the text.

The ion ratios are converted to equilibrium constants with eq 2, where

$$K_P^\circ = \frac{760 M^+(H_2)_n}{P_{H_2} M^+(H_2)_{n-1}} \quad (2)$$

P_{H_2} is the hydrogen pressure in Torr and $M^+(H_2)_n$ and $M^+(H_2)_{n-1}$ are the measured intensities of the cluster ions of interest. The standard free energy change is calculated with eq 3, where R is the gas constant and

$$\Delta G^\circ = -RT \ln K_P^\circ \quad (3)$$

T is the temperature. A plot of ΔG° *vs* temperature gives a straight line with intercept equal to ΔH_T° and slope equal to ΔS_T°, where T is the average experimental temperature (see Figure 1). This plot is functionally equivalent to a van't Hoff plot, but it is more convenient for our data analysis.

Data Analysis. In order to obtain the desired cluster bond dissociation energies (D_0), the ΔH_T° must be converted to ΔH_0° (≡ $-D_0$). This is done by calculating ΔG° as a function of temperature using statistical mechanics. In principle, all the bond lengths, frequencies, and the dissociation energy used in the calculation can be varied until the experimental and calculated ΔG° vs T functions agree. In practice, for all the systems studied to date, reasonably accurate theoretical geometries and vibrational frequencies were available for at least the first few clusters to guide the analysis. This is also true of the Sc^+–H_2 system where accurate geometries and frequencies have been calculated both by Rappe and Upton[16] and by Alvarado-Swaisgood and Harrison.[17] Estimating these parameters for the larger $Sc^+(H_2)_n$ clusters is discussed below. Because several low-frequency modes are present in the larger clusters, which could have a large effect on the cluster entropy, vibrational frequencies were varied over a wide range to see the effect on the resulting ΔH_0°. These uncertainties were included in the error limits.

The metal ion electronic entropy and enthalpy must also be included in the calculations. It has been shown that the M^+ spin–orbit states (J states) rapidly interconvert in collisions with He.[20] Presumably this interconversion also occurs in collisions with H_2. On this basis, a Boltzman population of J states was assumed (determined by the bath gas temperature). In the M^+H_2 cluster, both the inserted H–Sc^+–H ($^1A_1$,

(15) Sunderlin, L. S.; Armentrout, P. B. *J. Am. Chem. Soc.* **1989**, *111*, 3845.
(16) Rappe, A. K.; Upton, T. H. *J. Chem. Phys.* **1986**, *85*, 4400.
(17) Alvarado-Swaisgood, A. E.; Harrison, J. F. *J. Phys. Chem.* **1985**, *89*, 5198.
(18) Kemper, P. R.; Bowers, M. T. *J. Am. Soc. Mass Spectrom.* **1990**, *1*, 197.
(19) Kemper, P. R.; Hsu, M. T.; Bowers, M. T. *J. Phys. Chem.* **1991**, *95*, 10600.
(20) von Helden, G.; Kemper, P. R.; Hsu, M.-T.; Bowers, M. T. *J. Chem. Phys.* **1992**, *96*, 6591.

ground state) and the electrostatically bound (triplet) Sc^+H_2 had to be included to reproduce the experimental entropy. This point is discussed later.

Uncertainties. A number of potential sources of error are present in these experiments, e.g. pressure and temperature inaccuracies, quadrupole mass discrimination and resolution, collision-induced dissociation, and M^+ excited electronic states. The effects of these factors on our dissociation energies and entropies are discussed in refs 3 and 19. The net result is that the bond dissociation energies are essentially unaffected by these uncertainties. The entropies are affected to a small extent by any mass discrimination in the quadrupole mass analyzer, but in these experiments such mass discrimination is expected to be very small (given the parent/product mass difference of only 2 amu). Collision-induced dissociation (CID) of the clusters (as they are accelerated into the quadrupole) can also occur to a small extent for weakly bound clusters.[5,19] Such CID has a minor effect on measured values of ΔS°_T but essentially no effect on ΔH°_T. This effect is also expected to be small due to the small neutral mass and low collision energies (<0.2 eV c.m.). The amount of CID occurring must be small since in experiments where the cell pressure was changed by a factor of 3, the value of ΔG° showed no measurable change. This result argues against significant CID which should scale with cell pressure.

Excited electronic states must be considered in any measurement of transition metal ion reactivity. Deactivation of excited states was a concern in our experiments of Co^+ reacting with H_2.[3] The Co^+ ^3F and ^5F excited states are deactivated very slowly since they are bound very weakly to H_2. These weakly bound states prevent the attainment of the true, ground state first equilibrium at short reaction times. In contrast, the V^+ excited states were deactivated very efficiently in collisions with H_2,[4] and identical results were obtained with high-energy EI ionization and low-energy SI. Arrival time distributions (ATD's) in He of Sc^+ ions formed by electron impact (EI) showed a significant population of undeactivated, high-lying excited electronic states.[21] On the other hand, very little excited state Sc^+ (less than 1%) was seen when the Sc^+ ions were produced by SI[21] although greater than 11% excited Sc^+ is produced by SI ionization[14] at a filament temperature of 2300 K. This indicates that significant deactivation of the low-lying electronic states occurs in collisions with He. Since H_2 is expected to deactivate excited states more efficiently than He, it appears reasonable that Sc^+ is completely deactivated in the time scale of our experiments. To confirm this, ion chromatography experiments[1,2] were performed with EI and SI and found to give identical results. All of the results reported here were performed with the low-energy SI source.

An estimate of the absolute accuracy of our experimental entropy measurements can be made by comparison with theory. In several of these M^+·H_2 systems, very high level molecular structure calculations have been performed.[6-8] In these cases, the association entropies can be very accurately calculated. In all such cases, our experimental entropies are within ±1 cal/(mol·K) of the theoretical entropies. This probably is the best estimate of our maximum experimental error. The uncertainty in our enthalpy values is determined from the statistical variation between several data sets plus the possible range allowed by our statistical–mechanical fitting when extrapolating to $T = 0$. In all cases agreement between high-level ab-initio calculations and our experimental results is excellent, with the calculated D_0 values typically 85–90% of the experimental values. In the two cases where comparison with spectroscopic data is possible (Cr^+Ar[19] and Kr^+Ne[22]), the equilibrium results agreed with the spectroscopic results well within experimental error.

Reaction Rate. Rate coefficients were also determined for the first clustering reaction. Formation of the first ScH_2^+ cluster was very slow over the temperature range studied as shown in Figure 2. Quantitative rate coefficients can be obtained by modeling the approach to equilibrium assuming a simple bimolecular association mechanism (eq 4)

$$Sc^+ + H_2 \underset{k_b}{\overset{k_f}{\rightleftharpoons}} ScH_2^+ \qquad (4)$$

The resulting time dependent behavior of product ion/reactant ion ratios is shown in eq 5, where $(ScH_2^+/Sc^+)_t$ is the ratio of ScH_2^+ to Sc^+ at time

$$(ScH_2^+/Sc^+)_t = \frac{(ScH_2^+/Sc^+)_{eq}(1 - e^{-qt})}{[1 + (ScH_2^+/Sc^+)_{eq}e^{-qt}]} \qquad (5)$$

t, $(ScH_2^+/Sc^+)_{eq}$ is the final equilibrium ratio, $q = k_b + k_f[H_2]$, and $[H_2]$ is the concentration of H_2 in the drift cell. Both the concentration of H_2 and the equilibrium ratio $(ScH_2^+/Sc^+)_{eq}$ are known. The backwards rate k_b can be calculated with use of k_f and the equilibrium constant, K ($k_b = k_f/K$), and therefore the time dependence of our observed ion ratios can be fit by varying only the forward rate constant, k_f. Analysis of data such as that given in Figure 2a yields values of $k_f = 1.3 \times 10^{-16}$ cm^3/s at 260 K and 3×10^{-17} cm^3/s at 350 K, a substantial negative temperature dependence (see Figure 2b). These results will be discussed later in terms of a reaction mechanism.

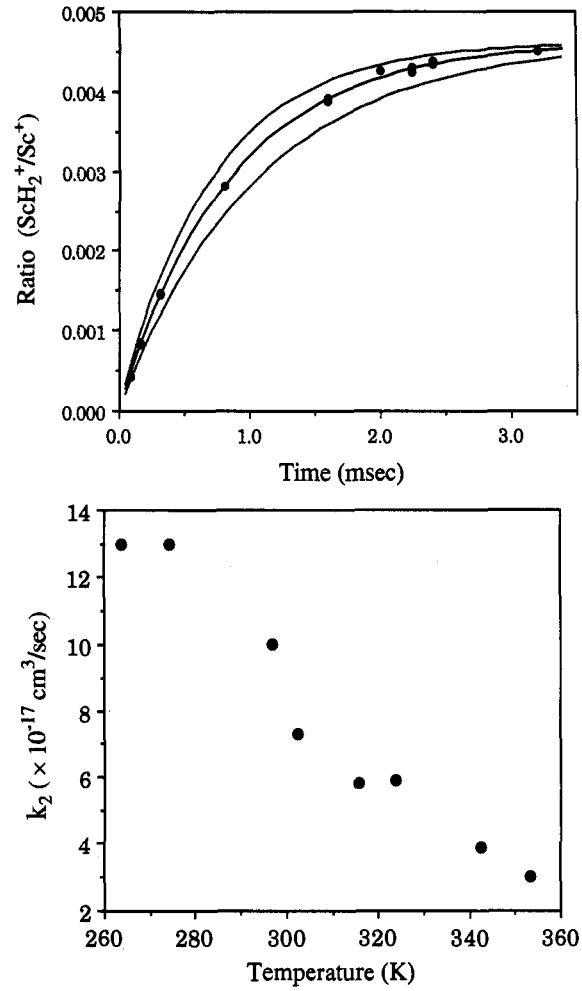

Figure 2. (a, top) A plot of the ratio of Sc^+H_2/Sc^+ *vs* time spent in the drift cell at $T = 300$ K and an H_2 pressure of 3 Torr. The data indicate the $Sc^+ + H_2 \rightarrow Sc^+H_2$ system approaches equilibrium only at very long times. The solid line through the points corresponds to a rate constant, k_f, for ScH_2^+ formation of 6×10^{-17} cm^3/s. The dotted lines above and below correspond to changes in k_f of ±20%. (b, bottom) A plot of the Sc^+H_2 formation rate constant, k_f, *vs* temperature. For details of the analysis see text. Note the very low reaction efficiency (the collision rate constant is about 1×10^{-9} cm^3/s). Also note the pronounced negative temperature dependence.

Computational Details

The primary objective of the electronic structure calculations is to facilitate the accurate analysis of the experimental results. We are therefore particularly interested in the structural properties of the different extrema on the potential energy surfaces (PES). As shown below, the dynamics of the insertion of Sc^+ into H_2 is a puzzling question. We have therefore examined the competition between the inserted (singlet) and non-inserted (singlet and triplet) pathways. As mentioned by Rappe and Upton,[16] only the behavior of the lowest lying asymptotes is of interest (namely $^{3,1}D$ (s^1d^1) and ^3F (d^2)). We have therefore only characterized the lowest energy complexes derived from these asymptotes.

(21) van Koppen, P. A. M., unpublished data, 1992.
(22) Kemper, P. R.; Bushnell, J. E.; Bowers, M. T. *J. Chem. Phys.* to be submitted for publication.

Table 1. Summary of Experimental Results

reaction	$-\Delta S^\circ_T$,[a] cal/(mol·K)	T,[b] K	$-\Delta H^\circ_T$,[a] kcal/mol	$-\Delta H^\circ_0$,[c] kcal/mol[c]
$Sc^+ + H_2 \rightarrow Sc^+(H)(H)$	19.1 ± 0.6[d]	308 (±45)	6.1 ± 0.2[d]	5.5 ± 0.3
$Sc^+(H)(H) + H_2 \rightarrow Sc^+(H)(H)(H_2)$	17.3 ± 1.1	290 (±40)	7.2 ± 0.3	6.4 ± 0.5
$Sc^+(H)(H)(H_2) + H_2 \rightarrow Sc^+(H)(H)(H_2)_2$	15.8 ± 0.5	250 (±50)	5.9 ± 0.2	5.4 ± 0.3
$Sc^+(H)(H)(H_2)_2 + H_2 \rightarrow Sc^+(H)(H)(H_2)_3$	17.9 ± 2.5	225 (±25)	5.5 ± 0.6	5.0 ± 0.6
$Sc^+(H)(H)(H_2)_3 + H_2 \rightarrow Sc^+(H)(H)(H_2)_4$	17.0[e]	201	4.9 ± 0.6[f]	

[a] Uncertainties are $\pm 2\sigma$ derived from a linear least-squares fit to data. [b] The temperature range is given in parentheses. [c] Includes uncertainty from fitting procedure. [d] These values include contributions from the non-inserted cluster, $Sc^+ \cdot H_2$. See text. [e] Entropy estimated. [f] Calculated from a single temperature with estimated entropy.

Ab initio electronic structure calculations were carried out with the Gaussian 92 program.[23] The geometries of the singlet and triplet states of the $Sc^+(H_2)_n$ complexes were optimized and the vibrational frequencies computed at the MP2 level. Spin-unrestricted canonical orbitals were used for the open-shell systems and only the valence electrons were correlated.

The Sc^+ basis set is the Wachters' (14s9p5d) primitive[24] set contracted as [8s4p3d]. Two diffuse p and one diffuse d are added, as recommended by Hay,[25] and the exponent of the single f gaussian ($\alpha = 1.0$) has been taken from Harrison. The final contraction is of the form (14s11p6d1f)/[8s6p4d1f]. The H basis is derived from the scaled (4s)/[2s] set of Dunning and Hay,[26] supplemented by a diffuse s ($\alpha = 0.071$) and three p functions ($\alpha = 1.2$, 0.40, and 0.13). This basis set has been optimized by Maitre and Bauschlicher[8] for the electrostatic interaction of H_2 with a transition metal cation.

The major weakness of this level of calculation is the relatively low level of electronic correlation which leads to an overestimation of the stability of the high-spin compared to the low-spin states and of the s^1d^n electronic configurations compared to the d^{n+1} electronic configurations.[27] Nevertheless, when the bonding is mainly electrostatic, these two defects can be reasonably well corrected. The energy of each electrostatic complex is calculated relative to its own asymptote. Then, since charge transfer between Sc^+ and the H_2 moieties is relatively small, we can approximate the energy shift for the electrostatic complex as the energy shift at its asymptote. Therefore, the absolute energy of each complex is estimated by correcting the UMP2 calculated energy by the error made at the asymptote limit $Sc^+ + H_2$. Previous ab initio electronic structure calculations have shown that the UMP2 wave function leads to reasonable geometries as well as frequencies for the electrostatic $M^+(H_2)_n$ complexes.[8] With respect to energy, calibration calculations of UMP2 against MCPF and CCSD(T) in larger basis sets showed that the expected underestimation of the binding energy is about 3.5 kcal/mol for $3d^n$ M^+ centers.

The energetics of the insertion of Sc^+ into H_2 has been accurately calculated by Rappe and Upton[16] and Alvarado-Swaisgood and Harrison,[17] and we used this value in our analysis to position the inserted product relative to the ground state asymptote. However, the bonding of the subsequent H_2 ligands to this inserted product is mostly electrostatic, and we therefore expect that the UMP2 calculated values are as accurate for the inserted $Sc^+(H)_2(H_2)_{n-1}$ as for the non-inserted $Sc^+(H_2)_n$ complexes.

Results and Discussion

The observed free energy ΔG° *vs* temperature data for $Sc^+(H_2)_n/Sc^+(H_2)_{n-1}$ (n = 1–4) equilibria are plotted in Figure 1. [Note: Even though Sc^+ is inserted into the first H_2 ligand, sometimes the sequential addition of H_2 will be designated with use of this structurally nonspecific notation for simplicity.] This functional form, rather than the usual van't Hoff plot, is used to facilitate the statistical mechanical analysis. As noted, the association enthalpies (ΔH°_T) and entropies (ΔS°_T) are given by the intercepts and slopes, respectively. These quantities, as well as the ΔH°_0, determined by using the statistical-mechanical procedures discussed above, are listed in Table 1. In the following sections we will discuss the five clusters formed starting with $Sc^+(H_2)$ and proceeding to $Sc^+(H_2)_5$.

Sc^+H_2. (a) Structure. Geometries and frequencies for the inserted H–Sc^+–H ion were taken from the calculations of Rappe and Upton[16] and Alvarado-Swaisgood and Harrison.[17] They find the Sc^+–H bond lengths to be 1.746 Å and the H–Sc^+–H bond angle to be 106.7°. The calculated frequencies are 1734, 1745, and 489 cm^{-1}. It should be noted that our MP2 optimized geometry (Sc^+–H bond length of 1.742 Å with a bond angle of 110.5°) is close to the above value. Our calculated frequencies (1732, 1814, and 523 cm^{-1}) are, as expected, generally higher than those obtained with a higher level of correlation. This supports our argument that the UMP2 calculations should give an accurate description of the subsequent electrostatic binding of H_2 units to the H–Sc^+–H skeleton.

The uninserted Sc^+H_2 complexes have also been considered. These clusters can be formed from any of the three lowest asymptotes ($^{3,1}D$ (s^1d^1) and the ^3F (d^2)). The UMP2 geometries and binding energies for one representative of each type of electrostatic complex are given in Figure 3. At the UMP2 level, the optimized bond length of the free H_2 molecule is 0.739 Å and the calculated H–H harmonic vibrational frequency is 4522 cm^{-1}. As shown in Figure 3, the H_2 ligand is basically unperturbed when it is bound to Sc^+, although the H_2 bond is slightly longer when the metal cation has an electronic configuration d^2 rather than s^1d^1. This result is not surprising since the 3d orbitals are more compact than the 4s, leading to a significantly closer approach of the ligand and consequently a larger electrostatic interaction. This, in turn, leads to greater Sc^+ $3d\pi \rightarrow H_2\sigma^*$ and $H_2\sigma \rightarrow Sc^+$ $4s\sigma$ donation, both of which increase the H–H bond length.

Another expected consequence of the larger size of the 4s relative to the 3d orbital is that the electrostatic interaction of H_2 and Sc^+ with an s^1d^1 electronic configuration does not strongly depend on the orbital occupation of the 3d electron or upon the spin coupling between this 3d electron and the 4s electron. The UMP2 dissociation energies are about the same for the $^3D(s^1d^1)$ and $^1D(s^1d^1)$ electrostatic complexes (0.5 and 0.4 kcal/mol, respectively) while the $^3F(d^2)$-derived complex is bound by 5.0 kcal/mol according to the calculations. The structure of the lowest state derived from each of the s^1d^1 asymptotes is shown in Figure 3. For the singlet state it is more favorable to singly occupy the in-plane $3d\pi$ orbital since it leads to some back donation

(23) Gaussian 92, Revision A, Frisch, M. J.; Trucks, G. W.; Head-Gordon, M.; Gill, P. M. W.; Wong, M. W.; Foresman, J. B.; Johnson, B. G.; Schlegel, H. B.; Robb, M. A.; Replogle, E. S.; Gomperts, R.; Andres, J. L.; Raghavachari, K.; Binkley, J. S.; Gonzalez, C.; Martin, R. L.; Fox, M. A.; Defrees, D. J.; Baker, J.; Stewart, J. J. P.; Pople, J. A.; Gaussian, Inc.: Pittsburgh, PA, 1992.
(24) Wachters, A. J. H. *J. Phys. Chem.* **1970**, *95*, 1033.
(25) Hay, P. J. *J. Phys. Chem.* **1977**, *66*, 4377.
(26) Dunning, T. H.; Hay, P. J. In *Methods of Electronic Structure Theory*; Schaefer, H. F., Ed.; Plenum Press: New York, 1977; pp 1–27.
(27) Bauschlicher, C. W.; Partridge, H. *Theor. Chim. Acta* **1993**, *86*, 13.
(28) Armentrout, P. B.; Kickel, B. In *Organo-metalic Ion Chemistry*; Freiser, B. E., Ed., in press.
(29) Schilling, J. B.; Goddard, W. A.; Beauchamp, J. L. *J. Phys. Chem.* **1987**, *91*, 5616.
(30) Petterson, L. G. M.; Bauschlicher, C. W.; Langhoff, S. R.; Partridge, H. *J. Chem. Phys.* **1987**, *87*, 481.

Table 2. UMP2 Vibrational Frequencies for $Sc^+\cdot(H_2)_n$ Complexes[a,b]

ion		Sc^+–H str	H–Sc^+–H bend	Sc^+–H_2 sym str	Sc^+–H_2 asym str	H_2–Sc^+–H_2 bend	H_2 int rot.	H–H str
$Sc^+\cdot H_2$	^3F			503	950			4034
	$^1D^c$			169	408			4409
	$^3D^d$			110	376			4433
$Sc^+\cdot(H_2)_2$	$^1D^{c,e}$			133	553	150	90	4398
				223	562	205		4398
	$^3D^{d,e}$			50	332	15	97	4459
				76	338	53		4460
$H-Sc^+-H$		1732	529					
		1814						
$H-Sc^+\cdot H_2$		1730	538	483	732	40	216	4345
		1805				100		
$H-Sc^+\cdot(H_2)_2$		1725	539	462	733	i22, i29	194	4346
		1793		496	734	27, 123	246	4348
$H-Sc^+\cdot(H_2)_3$		1716		430	649	i40, 34	i177	4332
			551	477	777	39, 73	276	4334
		1774		519	780	145, 146	344	4372

[a] In units of cm^{-1}. [b] UMP2 frequencies should be accurate. [c] First excited state 4s3d configuration. [d] Ground state 4s3d configuration. [e] D_{2h} symmetry.

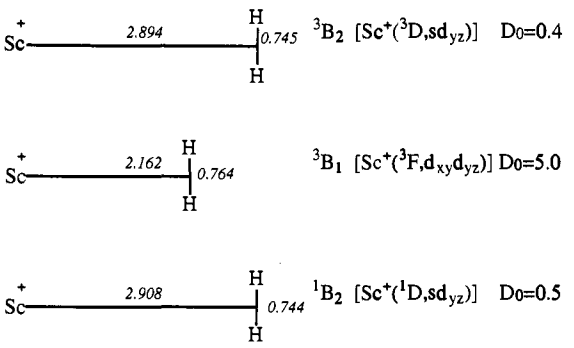

Figure 3. Calculated structures of the electrostatically bound Sc^+–H_2 complexes for the three lowest asymptotic electronic states of Sc^+. The structures and the binding energies were determined at the UMP2 level with a large basis set (see the text). The bond lengths are given in Å and the D_0 values in kcal/mol. This level of theory is expected to underestimate D_0 by about 3.5 kcal/mol for the d^2 state and by about 1.5 kcal/mol for the s^1d^1 states (see text).

into the H_2 σ^* orbital. However, this single-electron back-donation is unfavorable when the 4s and 3d electrons are high-spin coupled and the singly occupied 3d orbital in the ground state is a 3dδ orbital. This result is consistent with the recent calculations of Maitre and Bauschlicher[7] on the V^+ complexes: the single-electron donation from a 3d orbital into the H_2 σ^* orbital is unfavorable since it leads to a diminution of the 3d–3d exchange energy. This effect is less important in the present case since the 4s–3d exchange in the Sc^+ (^{3}D) is smaller than the 3d–3d exchange energy in the $^5D(d^4)$ ground state of V^+. This point is confirmed by the UMP2 geometry optimization of other states derived from the ^{3}D asymptote; the energy splitting between these states is less than 1 kcal/mol. The same procedure applied to the s^1d^1 singlet states shows that the energy splitting is probably slightly larger than 1 kcal/mol.

As mentioned above, UMP2 is known to underestimate the electrostatic binding energy of H_2 to a transition metal cation. This error has been estimated to be 3.5 kcal/mol in the case of $V^+(H_2)_{1,2}$ complexes,[7] where the electronic configuration on the metal cation is d^4. Using this correction, we can get a reasonable estimate of the actual binding energy of the $^3F(d^2)$ ($D_0 = 5 + 3.5 = 8.5$ kcal/mol). We should note that this correction is probably too high since our basis set includes a set of polarization functions. The accuracy of the UMP2 calculations for the s^1d^n configuration has been estimated here by a single point energy calculation with use of the CCSD(t) wave function. The calculated increase of the binding energy is 1 kcal/mol, and we estimate that the saturation of the basis set might lead to a further increase of the binding energy by 0.5 kcal/mol at most. Therefore, the correction energy applied to the s^1d^1 binding energy is 1.5 kcal/mol, leading to approximately 2.0 kcal/mol for the binding energy of the ^{3}D and ^{1}D s^1d^1 complexes.

(b) Thermochemistry. The ground state binding energy for the first H_2 molecule to Sc^+ was determined to be 5.5 ± 0.3 kcal/mol (Table 1). The very slow approach to equilibrium (see Figure 2) coupled with predictions from theory argue strongly that this ground state association product is the inserted H–Sc^+–H species. The 5.5 kcal/mol binding energy thus corresponds to two scandium–hydride bonds with average binding energies of 54.4 ± 0.2 kcal/mol. In Table 3 existing literature results are listed along with the present values. Agreement is seen to be generally good. The estimate of Tolbert and Beauchamp[13] is in quite good agreement but the rather large uncertainties make quantitative comparison less meaningful. Armentrout and co-workers have made several determinations of the dissociation energy for the process

$$H\text{–}Sc^+\text{–}H \rightarrow 2H + Sc^+ \qquad (6)$$

by observing endothermic thresholds in the reactions of Sc^+ with H_2,[14] CH_4,[15] C_2H_6, etc.[11] These dissociation energies tend to be significantly higher than our result. One problem with the comparison is the uncertainty in the experimental temperature of the guided beam experiments. Recently Armentrout and Kickel have reexamined the guided beam data and converted the results to 0 K values.[28] The resulting agreement with the present work is better but still outside the combined uncertainties. Armentrout and Kickel note, however, that this may be due to small amounts of excited Sc^+ in the reactant beam which would reduce the observed onset.

Agreement between theory and our results is reasonably good.[16,17] Although both theoretical studies predict the H–Sc^+–H ($^1A_1$) inserted complex to be unbound with respect to the ground state reactants (Sc^+ ^{3}D and H_2), this is due to differential accuracy in the computations. The dissociation of H_2 (D_0 for H–H → 2H•) is more accurately calculated than that of H–Sc^+–H (eq 6). The result is a biasing toward the stability of the $Sc^+ + H_2$ reactants. The calculated Sc^+–H bond strengths are quite good: 91.2% and 92.5% of the present experimental value (Table 3). Thus, in interpreting the theoretical ΔH calculations, it is useful to remember tha these are generally with reference to an internally calculated D_0 for H_2, rather than the experimental value.

As noted above, our analysis indicates that a significant amount of the uninserted first cluster is present over the temperature range of our measurements. This conclusion is based on a comparison between the calculated association entropy for the inserted cluster ($\Delta S° = -21.4$ cal/(mol·K)) and the experimental value ($\Delta S° = -19.1$ cal/(mol·K)). Since the entropy calculation

Table 3. Sc^+–$H_{1,2}$ Dissociation Energies

Sc^+–H[a]	H·Sc^+–H[b]	Sc^+–2H[b]	Sc^+–H_2[b]	ref source
			−5.5 ± 0.3	this work
56.2 ± 2.0[c]	55.4 ± 3.0[c]	111.6 ± 1.0[c]	−8.3 ± 1.0[c]	28
56.3 ± 2.0				14
57.2 ± 1.4				15
54.0 ± 3.5		115.5 ± 3.0	−12.1 ± 3.0	11
54.0 ± 4.0	54.0	108 ± 7	−4.8 ± 7	13
57.2	50.7	100.7	+0.3	17
50.8	50.7	101.5	+1.8	16
55.2				29
56.0				30

[a] Dissociation from the $^2\Delta$ ground state to yield ground state products. [b] Dissociation from the $^1A_1$ ground state of H–Sc^+–H to yield Sc^+(^{3}D) + H_2. [c] Values referenced to 0 K.

for the inserted species is tightly fixed by well-known molecular parameters, an unacceptably large amount of mass discrimination would be required to reconcile the experimental and theoretical entropy in the absence of other effects.

As shown by our ab initio calculations, the electrostatic complex derived from the ^{3}D asymptote (estimated D_0 = 2.0 kcal/mol) is less strongly bound than the inserted species (experimental D_0 = 5.5 kcal/mol). Considering these enthalpies, it might seem that only a negligible amount of uninserted $Sc(^3D)^+H_2$ would be present at equilibrium. In fact, significant amounts of the uninserted complex are present at high temperatures due to the much less negative ΔS associated with the formation of uninserted $Sc(^3D)^+H_2$ relative to H–Sc^+–H. The larger entropy for Sc^+H_2 is due to the lower vibrational frequencies and longer Sc^+–H bond length of the electrostatic complex and also to its large electronic "degeneracy". The degeneracy of $Sc^+[^3D\ (s^1d^1)]$ is 15, and since the single occupation of the diffuse 4s orbital dictates the structural and energetic characteristics of the bonding, the $Sc^+(^3D)H_2$ complex should also have an electronic degeneracy of 15 (i.e., different orbital occupations of the 3d electron do not affect the bonding). The resulting ΔS for such a complex is about −14 cal/(mol·K), compared with −21.4 cal/(mol·K) associated with the formation of the inserted species. Since the entropies of both the inserted and non-inserted complexes are fairly accurately known, the experimental data can be fit by using only the binding energy of the non-inserted cluster as a parameter. Such a fit yields D_0 = 2.1 ± 0.5 kcal/mol for the non-inserted cluster, in good agreement with the theoretical estimate described above. Under these conditions the (Sc^+ + H_2) cluster product is ~100% inserted at temperatures below ~200 K and is ~50% inserted at a temperature of 460 K. The important point is that varying all of the unknown parameters over their entire range of reasonable values changes the final value of D_0 for the inserted complex by only a few tenths of a kilocalorie per mole. The uncertainty in D_0 for the non-inserted complex is larger for two reasons. First, it is populated only at high temperatures and the extrapolation to 0 K is less certain. Second, the uncertainty in the low-frequency vibrations leads to larger error limits.

There are many previous determinations of the first Sc^+–H bond energy[11-17,28-30] (both experimental and theoretical, see Table 3). There is agreement that the ground state is $^2\Delta$ and that the bond strength is close to 55 kcal/mol. This implies that the first and second hydride bond strengths are nearly equal (since from our data the average H–Sc^+ bond strength in H–Sc^+–H is 54.4 kcal/mol) and that the second bond may actually be slightly weaker than the first. This is perhaps surprising since it has been argued that the second hydride bond should be stronger as the loss of d–s exchange energy occurs in forming the first hydride bond.[13]

(c) Reaction Mechanism. There are two facts that need to be explained by any proposed mechanism: first the reaction efficiency for forming the first cluster is extremely low (on the order of 10^{-7} per collision), and second this reaction efficiency *decreases* as temperature increases. While the extremely low reaction efficiency is consistent with some kind of energy barrier, the negative temperature dependence is not. The calculations of Rappe and Upton[16] strongly support a barrier along the reaction coordinate as shown in the reaction coordinate diagram of Figure 4. These authors show the $3d^2$ ^{1}D third excited state of Sc^+ diabatically correlates to inserted H–Sc^+–H products via a forbidden crossing with the lower energy 4s3d ^{1}D asymptotic state and a spin–orbit coupled crossing to the ground 4s3d ^{3}D asymptotic state. The net effect is a barrier of about 20 kcal/mol with respect to the Sc^+ ground state. When the overall accuracy of the calculation is considered, this barrier may well be too high by 8–10 kcal/mol, but the important point is a substantial barrier definitely exists on the Sc^+ + H_2 surface.

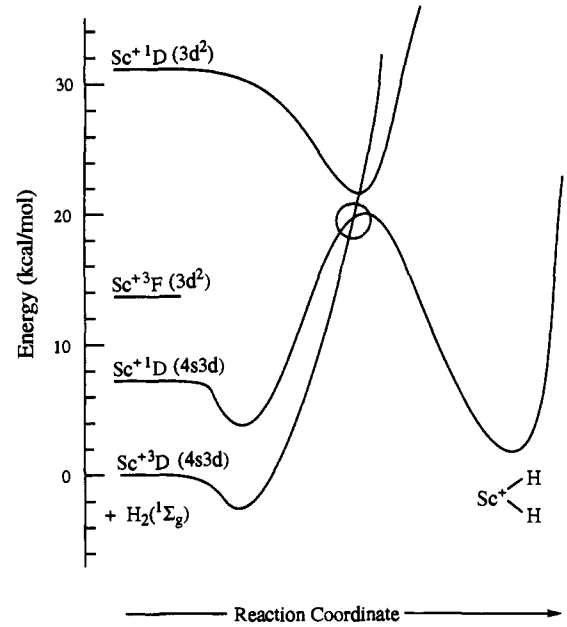

Figure 4. Potential energy surfaces modeled after the results of Rappé and Upton (ref 16) for the C_{2v} approach of Sc^+ to H_2. The two ^{1}D states undergo an avoided crossing, allowing a relatively low energy entry to the inserted complex. The circle denotes a spin–orbit coupled crossing between the ^{3}D ground state and the ^{1}D first excited state. In this model the ^{3}F ($3d^2$) state does not enter into the insertion process. The state designations correspond to the asymptotic Sc^+ states.

The usual requirement for negative temperature dependence is to have the rate determining transition state be at slightly lower energy than the asymptotic energy of the ground state. If the uninserted $Sc^+(H_2)_n$ clusters are considered, it is clear that this can occur. Rappe and Upton did not explore these electrostatically bound complexes that occur at relatively large values of Sc^+–H_2 separation. We have examined these theoretically for one and two H_2 additions to the three lowest energy states of Sc^+ (see Figures 3 and 5). The important finding is that addition of H_2 molecules to these states leads to a lowering of the insertion barrier *relative to the asymptotic energy of the ground state* [4s3d ^{3}D Sc^+ + nH_2]. Since the $3d^2$ ^{3}F state is stabilized by ~6 kcal/mol per H_2 ligand relative to the 4s3d states, it becomes the lowest energy state upon addition of three H_2 molecules. Further, since only d electrons are present on the metal for this state, the H_2 molecules are about 0.7 Å closer to the Sc^+ center than analogous H_2 molecules on 4s3d sites (see Figures 3 and 5). This will further lower the barrier. Finally, addition of the third H_2 ligand appears to provide sufficient stabilization energy to bring the insertion barrier *below* the asymptotic energy of the [4s3d ^{3}D Sc^+ + $3H_2$] ground state. The net effect is that low-energy insertion of Sc^+ into an H–H bond occurs only after three H_2 ligands are bound to the Sc^+ center. The schematic potential energy surfaces analogous to those shown in Figure 4 for Sc^+ + H_2 are shown in Figure 6 for sequential

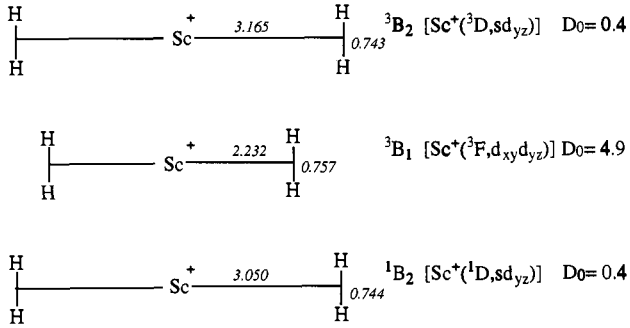

Figure 5. Calculated structures of the electrostatically bound $Sc^+(H_2)$ complexes for the three lowest energy asymptotic states of Sc^+. The structures and binding energies were determined at the UMP2 level (see text). The bond lengths are in Å and the binding energies in kcal/mol are for loss of one H_2 ligand.

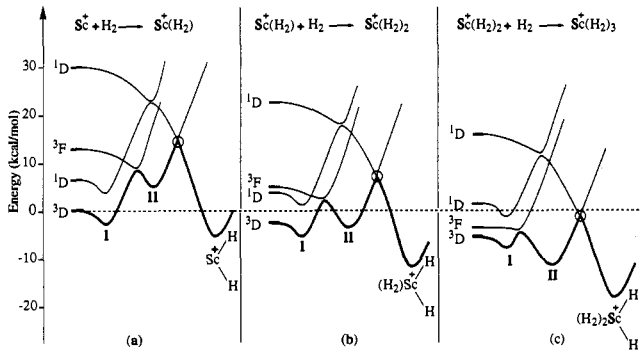

Figure 6. Schematic potential energy surfaces for the sequential addition of three H_2 molecules to the four lowest energy states of Sc^+. In frame a the term symbols ^{3}D, ^{1}D, ^{3}F, and ^{1}D represent the actual electronic states of Sc^+. In frame b these term symbols are associated with ScH_2^+ molecules that would asymptotically dissociate to the appropriate Sc^+ state. The initial energies in frame b correspond to the energies associated with the four Sc^+H_2 electrostatically bound complexes. Similar considerations hold for frame c, except the initial energies correspond to $Sc^+(H_2)_2$ electrostatically bound complexes. The symbols I and II correspond to the electrostatic complexes formed by sequential addition of H_2 to $Sc^+(^3D)$ and $Sc^+(^3F)$, respectively. The circle represents the spin–orbit crossing between the state associated with asymptotic ^{3}F Sc^+ and the higher energy ^{1}D state. Of importance is the fact that this crossing drops below the ground state energy after electrostatic addition of three H_2 ligands thus allowing thermal energy access to the inserted complex. The darkened line symbolizes the adiabatic formation of the inserted complex in frames (a), (b) and (c).

Scheme 1

$$Sc^+(4s3d\ ^3D) \underset{-H_2}{\overset{+H_2}{\rightleftharpoons}} Sc^+(^3D)H_2 \underset{-H_2}{\overset{+H_2}{\rightleftharpoons}} Sc^+(^3D)(H_2)_2 \underset{-H_2}{\overset{+H_2}{\rightleftharpoons}} Sc^+(^3D)(H_2)_3$$

$$Sc^+(^3D)(H_2)_3 \circlearrowright Sc^+(d^2\ ^3F)(H_2)_3 \circlearrowright \begin{matrix} H \\ H \end{matrix}\!\!> Sc^+(^1A_1)(H_2)_2$$

$$\begin{matrix} H \\ H \end{matrix}\!\!> Sc^+(H_2)_2 \underset{+H_2}{\overset{-H_2}{\rightleftharpoons}} \begin{matrix} H \\ H \end{matrix}\!\!> Sc^+(H_2) \underset{+H_2}{\overset{-H_2}{\rightleftharpoons}} H\text{–}Sc^+\text{–}H$$

additions of H_2 molecules up to $Sc(H_2)_3^+$. Phenomenologically, the sequence of events is depicted in Scheme 1. In this scheme, the electronic states depicted correspond to the asymptotic states of Sc^+ with the exception of the inserted cluster, where the $Sc^+(H)_2$ state symmetry is given. Once the stable inserted species is formed it will rapidly equilibrate, forming the various structures from H–Sc^+–H to H–Sc^+–$H(H_2)_3$ given in Figure 7. It is not clear whether or not the $Sc^+(^3D)(H_2)_3$ and $Sc^+(^3F)(H_2)_3$ clusters are long lived or whether the isomerization to the inserted species is very rapid once the H_2 ligand approaches $Sc^+(^3D)(H_2)_2$. It is probable these ions do not equilibrate with $Sc^+(^3D)(H_2)_2$, and hence a "short" arrow is shown for the dissociation of $Sc^+(^3D)(H_2)_3$. Regardless, the $Sc^+(^3D)(H_2)_2$ cluster is the reactant ion responsible for the formation of the inserted H–Sc^+–$H(H_2)_2$ cluster and consequently H–Sc^+–H itself.

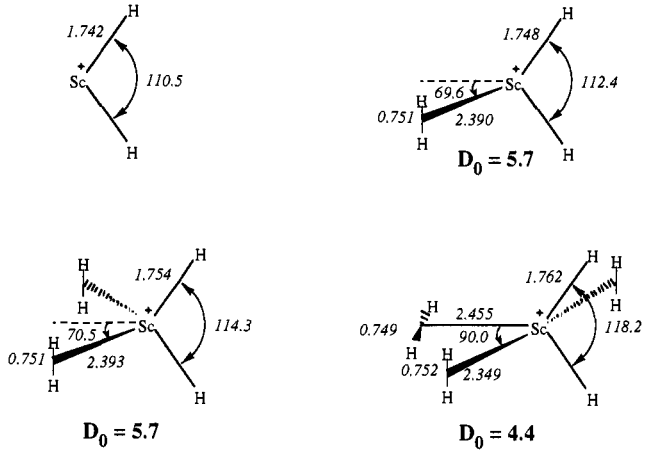

Figure 7. Calculated structures of the lowest energy inserted H–Sc^+–H complexes with 0, 1, 2, and 3 H_2 ligands attached. The structures and binding energies were determined at the UMP2 level. The bond lengths are in Å, the angles in deg, and the values of D_0 in kcal/mol.

The mechanism in Scheme 1 readily explains both the negative temperature dependence and the apparent inefficiency in the formation rate of the inserted H–Sc^+–H cluster. What must be kept in mind is the experimental data reported in Figures 2 and 3 are for phenomenological reaction 4. However, as we have discussed, this mechanism cannot be correct. In Scheme 1 the first two equilibria occur quickly and serve to transform a small fraction of the $Sc^+(^3D)$ ions into $Sc^+(^3D)(H_2)_2$ clusters. We believe this cluster is the actual reactant ion. As shown in panel c of Figure 6, there is still a barrier to reaction for the step

$$Sc^+(^3D)(H_2)_2 + H_2 \rightarrow H\text{–}Sc^+H(H_2)_2 \qquad (7)$$

with an activation energy E^*. Hence, if we could observe reaction 7 directly it would have a positive temperature dependence with $k \propto \exp(-E^*/RT)$. In our experiment, however, we can only observe the $Sc^+ + H_2 \rightarrow$ H–Sc^+H reaction, and hence the temperature dependence of the fractional abundance $[Sc^+(H_2)_2]/Sc^+$ must also be taken into account. Since Sc^+ and $Sc^+(H_2)_2$ are in equilibrium, this ratio is simply given by $[Sc^+(H_2)_2]/Sc^+ \propto \exp(TBE/RT)$ where TBE is the energy required for $Sc^+(H_2)_2 \rightarrow Sc^+ + 2H_2$. It follows that $k_{obs} \propto \exp[(TBE - E^*)/RT]$. Hence, a negative temperature dependence will result if $|TBE| > |E^*|$. This condition holds for $Sc^+(H_2)_2$ but not for $Sc^+(H_2)$, as shown in Figure 6. This requirement is also just another way of saying the barrier to insertion must fall below the asymptotic energy of $Sc^+(^3D) + nH_2$ shown by the dotted line in Figure 6. The same considerations also explain the apparent great inefficiency of phenomenological reaction 4 since the ratio $[Sc^+(H_2)_2/Sc^+]$ is of the order of 10^{-6} for the temperature range of our experiments.

Finally, the fine details of the isomerization dynamics of $Sc^+(^3F)(H_2)_3 \rightarrow$ H–$Sc^+(^1A)H(H_2)_2$ cannot be accurately assessed at this time and await some sophisticated, high-level, electronic structure calculations and perhaps dynamics calculations as well. The surface hopping at the spin–orbit coupled transition state may also have a temperature dependence that could augment the one discussed in the previous paragraph. It should also be noted that the final two equilibria in Scheme 1 that transport H–Sc^+H-$(H_2)_2$ to H–Sc^+H occur on a time scale too short to measure in our experiment and do not affect the kinetics discussed above.

Sc^+·$(H_2)_2$. (a) Structure. We have examined both inserted (one inserted and one uninserted H_2) and fully uninserted complexes, and the present calculations show that the lowest energy structure corresponds to one dihydrogen ligand electrostatically bound to the inserted H–Sc^+–H molecule. The uninserted cluster (both H_2 ligands bound electrostatically) is much higher in energy (compare Figures 5 and 7) and the

Table 4. Binding Energies[a] ($-\Delta H_0^\circ$) for the Equilibrium $M^+(H_2)_{n-1} + H_2 \rightleftharpoons M^+(H_2)_n$

n	$-\Delta H_0^\circ(K^+)$[c]	$-\Delta H_0^\circ(Sc^+)$[b,d]	$-\Delta H_0^\circ(Ti^+)$[e]	$-\Delta H_0^\circ(V^+)$[f]	$-\Delta H_0^\circ(Co^+)$[g]
1	1.45 ± 0.2	5.5 ± 0.3[h] (2.1 ± 0.5)[i]	7.5 ± 0.3	10.2 ± 0.5	18.2 ± 1.0
2	1.35 ± 0.4	6.9 ± 0.3	10.0 ± 0.3	10.7 ± 0.5	17.0 ± 0.7
3		5.4 ± 0.3	9.3 ± 0.4	8.8 ± 0.4	9.6 ± 0.5
4		5.0 ± 0.4	9.4 ± 0.5	9.0 ± 0.4	9.6 ± 0.6
5		~4.4[j]	9.7 ± 0.5	4.2 ± 0.3	4.3 ± 0.5
6			9.5 ± 0.5	9.6 ± 0.5	4.0 ± 0.5

[a] In units of kcal/mol. [b] For Sc^+, the $n = 1$ species is H–Sc^+–H and subsequent H_2 ligands are added as dihydrogen. [c] Reference 5. [d] This work. [e] Reference 31. [f] Reference 4. [g] Reference 3. [h] For formation of the inserted H–Sc^+–H molecule. [i] For formation of the electrostatically bound $Sc^+ \cdot H_2$ cluster that asymptotically correlates to the $3d^14s^1$ ^3D ground state of Sc^+. [j] Estimated from a single measurement, see text.

equilibrium population is negligible (it is, however, important to the mechanism of insertion, see above).

We first characterized the two C_{2v} isomers of the inserted product, where H_2 attaches opposite to the two hydrides. In the lowest energy structure, the electrostatically bound H_2 eclipses the two Sc–H bonds, but the staggered conformation is only 0.6 kcal/mol higher in energy. The energy difference might be due to the slight donation from the metal (antisymmetric combination of the two Sc–H bonds, b_2 symmetry) into the σ^* orbital in the eclipsed conformation while no such donation is possible in the staggered conformation. However, neither of these two C_{2v} conformers is a minimum on the PES. The eclipsed conformation has one imaginary frequency, and geometry optimization along the vibrational mode responsible for the imaginary frequency leads to a C_s minimum on the PES where the Sc–H_2 plane forms an angle of 70° with respect to the H–Sc–H plane and the second H–H bond axis is parallel to this plane (Figure 7). The stabilization energy of the eclipsed C_{2v} conformer relative to the staggered isomer (0.4 kcal/mol) is again rather small, indicating that charge transfer is small, and that destabilization of the eclipsed structure is due to the repulsion between the H_2 σ orbital and the symmetric combination of the two Sc–H bonding orbitals. This repulsion is rather weak, however, and the gradient of the potential with respect to the out-of-plane angle is small. The result is two very low frequency bending modes as well as a nearly free internal rotation of the uninserted H_2 ligand. These parameters are listed in Table 2.

(b) Thermochemistry. Our statistical-mechanical analysis shows the uninserted H_2 ligand is bound by 6.4 ± 0.5 kcal/mol. The binding energy (D_e) from our ab-initio calculations is 7.3 kcal/mol, yielding a theoretical value of D_0 = 5.4 kcal/mol, or 84% of the experimental value. Unlike the covalent scandium–hydride bonds in the inserted cluster, the second H_2 is bound almost exclusively by electrostatic forces. This bonding is similar to that in previous M^+H_2 systems,[3-5,31] and in Table 4 we compare second H_2 cluster bond energies for the $K^+/Sc^+/Ti^+/V^+$ and Co^+ systems. These data show that the electrostatic binding energies increase monotonically with atomic number in the first part of this transition series. We believe this is due largely to the variation in the size of the core electron cloud. In all these systems (except Co^+) the H_2 ligands approach an empty dσ orbital and the resulting bond length is largely controlled by repulsion between the H_2 and the core electrons. As the atomic number increases, the size decreases,[32] the bond length decreases, and a stronger attraction results. The effect is strong due to the r^{-4} or r^{-3} variation in electrostatic attraction (charge-induced dipole or charge-quadrupole potentials, respectively). An even stronger variation with nuclear charge would be found were it not for repulsion between the H_2 ligands and the dπ orbitals in Ti^+ and V^+. In the K^+ clusters, the dπ orbitals are empty; in the Sc^+ clusters, the valence electrons are localized in the Sc–H bonds and the dπ orbitals are essentially empty. In the Ti^+ and V^+ systems, however, the H_2 ligands must approach a half-filled dπ orbital. A close approach results in d$\pi \rightarrow \sigma^*$ back-donation which in these ions results in a loss of d–d exchange energy and is unfavorable. In ions with a filled dπ orbital (e.g. Co^+) this back-donation *increases* the d–d exchange and is favorable. This effect is largely responsible for the increase in binding energy between V^+ and Co^+ (Table 4).

Table 1 shows that the ΔS for the second association is more positive than that for the first clustering reaction (–18.6 cal/(mol·K) vs –19.1 cal/(mol·K)). (Remember that the ΔS for formation of the pure inserted cluster is –21.4 cal/(mol·K), even more negative.) The difference in the second clustering entropy is due in part to an increase in the rotational moments of inertia of the larger cluster but primarily to the low-frequency vibrations (bending modes) present in $Sc^+(H)_2H_2$ but absent in the inserted $Sc^+(H)_2$ molecule.

$Sc(H_2)_3$. (a) Structure. Three high-symmetry structures were initially investigated. Two conformers with T_d symmetry were found to be very close in energy (ΔE = 0.8 kcal/mol), while a quasi-square-planar conformer is higher in energy (4.5 kcal/mol above the lowest energy T_d isomer). The lowest energy structure (Figure 7) has C_{2v} symmetry with the two electrostatically bound H_2 ligands parallel to the H–Sc^+–H plane and a H_2–Sc^+–H_2 included angle equal to 141°. The calculated values for the Sc–H_2 bond lengths are both 2.39 Å. Again the small energy difference between the two T_d symmetry isomers and the two small imaginary frequencies (29 and 22 cm^{-1}) of these species show that the H_2 internal rotations are essentially free.

(b) Thermochemistry. The third H_2 ligand is again bound primarily by electrostatic forces. The experimental binding energy is 5.39 ± 0.3 kcal/mol and our ab initio binding energy is 5.7 kcal/mol. Given the similar mode of binding in the second and third clusters, the decrease in binding energy of the third H_2 may seem surprising. The comparison data in Table 4 show, however, that a decrease is expected. Further, the data show that the stronger the binding of the first two ligands, the greater is the expected decrease. We believe this is due largely to simple steric repulsion between the ligands. Typically, the first two ligands attach on opposite sides of the molecule with very little interaction. The third ligand then attaches somewhere between, interferes with both, and is thus bound less strongly. If the first two ligands are strongly bound, the bond distances are smaller and the steric interference is greater when the third ligand is added. The data for the $Sc^+(H)_2(H_2)_2$ cluster follow this trend.

The ΔS is more positive for the third clustering reaction than the second (–15.6 cal/(mol·K) vs –18.6 cal/(mol·K)). This is again due to increases in the positive vibrational and rotational entropies.

$Sc^+(H_2)_4$. The structure for this cluster was determined to be a quasi-trigonal-bipyramid. The two Sc^+–H bonds and one of the Sc^+–H_2 bonds form the triangular base with the H–H bond axis of the dihydrogen ligand perpendicular to the H–Sc–H plane. The other two H_2 ligands are then added above and below and the resulting symmetry is C_{2v}. The calculated bond lengths are given in Figure 7.

The experimental bond strength is 5.0 ± 0.4 kcal/mol, slightly less than that of the third cluster (5.4 kcal/mol). Again this is expected due both to the increased steric interference between ligands and the resulting displacement of the first two H_2 ligands from their optimal positions. The association entropy is also more negative which may indicate a general "tightening" of the modes for the same reason. The essentially free internal rotations in the smaller clusters could be lost, for example.

$Sc^+(H_2)_5$. The fifth cluster was observed only at the lowest experimental temperature (200 K). On the basis of an estimated

(31) Bushnell, J. E.; Kemper, P. R.; Bowers, M. T. *J. Phys. Chem.*, to be submitted for publication.

(32) Barnes, L. E.; Rosi, M.; Bauschlicher, C. W. *J. Chem. Phys.* **1990**, *93*, 609.

entropy of ~17 cal/(mol·K), the bond strength is expected to be about 4.4 kcal/mol. The addition of the sixth H_2 ligand was not observed under our experimental conditions. This result is consistent with a first row "solvation shell" of six, where in the case of Sc^+ two of the ligands are H-atoms and four of them are H_2. All other first-row metals are observed to have solvation shells of six H_2 ligands.[3,4,31]

We have done ab initio calculations on $H–Sc^+–H(H_2)_4$. These calculations indicate that two H_2 ligands lie in the $H–Sc^+H$ plane, with the additional ligands above and below the plane, respectively. Hence, a quasioctahedral structure is formed. In the plane the $H–Sc^+–H$ angle is greater than 90°, and the $H_2–Sc^+–H_2$ angle is less than 90°. The estimated theoretical binding energy of the final H_2 ligand is ~4 kcal/mol.

Conclusions

We have made experimental determinations of binding energies and entropies for $Sc^+(H_2)_n$ (n = 1–5). The binding energy of the first cluster is in reasonable agreement with previous experimental results, as well as high-level ab initio calculations. However, the size of the binding energy, the very slow approach to equilibrium, and the negative temperature dependence of the formation rate coefficient strongly indicate Sc^+ is inserted into the first H_2 ligand and forms two covalent σ bonds with the H-atoms. For n = 2 and higher, the H_2 ligands are bound electrostatically (uninserted). These bond energies are largely determined by the size of the scandium ion and by steric interference between the H_2 ligands. A solvation shell of 6 is observed for Sc^+ (two H-atoms and four H_2 ligands) consistent with other first-row transition metals.

Ab initio calculations were done and reported on the higher order clusters to determine their geometries, bond lengths, and frequencies.

The observed reaction inefficiency and temperature dependence for formation of $Sc^+(H)_2$ indicate that the reaction surfaces which were determined in the calculations of Rappe and Upton may govern the insertion in a single collision environment, but that a different mechanism must operate in our high-pressure experiments. A mechanism involving uninserted H_2 ligands electrostatically bound to Sc^+ (in the ^3D and ^3F states) is proposed to explain our data. This mechanism indicates that the Sc^+ insertion is "cluster mediated", the first example for such a reaction in σ bond activation by a transition metal center. This mechanism could be tested with ab initio methods by evaluating the ^1D transition state for $Sc^+–H_2$ and/or $Sc^+(H_2)_2$ inserting into H_2 in order to determine the position at which the ^3D and ^3F surfaces cross the ^1D surface.

Acknowledgment. We gratefully acknowledge the support of the National Science Foundation under Grant No. CHE 91-19752. In addition, P.M. thanks CNRS (France) for financial support while on leave.